Artificial Intelligence in Medicine 78 (2017) 55–60

Contents lists available at ScienceDirect

Artificial Intelligence in Medicine

journal homepage: www.elsevier.com/locate/aiim

Automatic detection of surgical haemorrhage using computer vision

Alvaro Garcia-Martinez*, Jose María Vicente-Samper, José María Sabater-Navarro

Systems and Automatics Engineering Department, Miguel Hernández University, Avinguda de la Universitat d'Elx, Elche, 03202, Spain

ARTICLE INFO

Article history:
Received 15 December 2016
Received in revised form 2 May 2017
Accepted 5 June 2017

Keywords:
Computer vision
Laparoscopic surgery
Massive bleeding

ABSTRACT

Background and objectives: On occasions, a surgical intervention can be associated with serious, potentially life-threatening complications. One of these complications is a haemorrhage during the operation, an unsolved issue that could delay the intervention or even cause the patient's death. On laparoscopic surgery this complication is even more dangerous, due to the limited vision and mobility imposed by the minimally invasive techniques.
Methods: In this paper it is described a computer vision algorithm designed to analyse the images captured by a laparoscopic camera, classifying the pixels of each frame in blood pixels and background pixels and finally detecting a massive haemorrhage. The pixel classification is carried out by comparing the parameter B/R and G/R of the RGB space colour of each pixel with a threshold obtained using the global average of the whole frame of these parameters. The detection of and starting haemorrhage is achieved by analysing the variation of the previous parameters and the amount of pixel blood classified.
Results: When classifying in vitro images, the proposed algorithm obtains accuracy over 96%, but during the analysis of an in vivo images obtained from real operations, the results worsen slightly due to poor illumination, visual interferences or sudden moves of the camera, obtaining accuracy over 88%. The detection of haemorrhages directly depends of the correct classification of blood pixels, so the analysis achieves an accuracy of 78%.
Conclusions: The proposed algorithm turns out to be a good starting point for an automatic detection of blood and bleeding in the surgical environment which can be applied to enhance the surgeon vision, for example showing the last frame previous to a massive haemorrhage where the incision could be seen using augmented reality capabilities.

1. Introduction

On Minimally Invasive Surgery (MIS), haemorrhages remain one of the major complications present in all types of interventions, being particularly dangerous the Major Vascular Injuries (MVI). Nevertheless, it seems there is no global consensus to classify these complications [1].

Although there is not an extensive literature on the incidence of this problem, some authors have carried out some studies on the subject like Opitz et al. [2] whom analysed more than 43,000 interventions at Swiss hospitals and clinics, concluding that the incidence of bleedings on laparoscopic surgeries amounts 1.7% whereas the incidence of MVI amounts 0.09%.

Regarding abdominal surgery, more specifically laparoscopic surgery, we found a study of Opasanon et al. [3] which collect few previous studies providing an estimation of the incidence around 0.07–1.2%. It is especially interesting the study of Duca et al. [4], in which the authors analyse the complications occurred during 9542 laparoscopic cholecystectomies for a period of 9 years, concluding that the incidence of haemorrhages on laparoscopic surgeries amounts 2.3% and around 1.9% of the operations needs a conversion to open surgery of which 4.8% where a direct result of a bleeding.

Although these percentages may seem low, it is estimated around 10–15% of the population of a developed country will be diagnosed of gallstones and will required a surgical intervention. This means that in a country like USA where about 750,000 cholecystectomies are performed each year, of which near 90% uses MIS techniques, approximately 15,500 persons will suffer a haemorrhage during the surgery and 615 will require a conversion to open surgery due to this complication [5].

The consequences of a bleeding at a laparoscopic surgery can be just a simple delay of the intervention, a major recovery time at the hospital or even the death of the patient as Anna Mases et al. state in their study [6].

In general, most authors stress the importance of early detection of bleeding to alleviate their negative effects, therefore it is

* Corresponding author.
E-mail address: alvaro.garciam@umh.es (A. Garcia-Martinez).

http://dx.doi.org/10.1016/j.artmed.2017.06.002
0933-3657/

required a reliable system able to analyse the characteristics of this complication and detect it as soon as possible. Due to the proliferation of researches focused on the analysis of images provided by a laparoscopic camera like the described at [7], it was decided to design a computer vision algorithm able to detect an internal haemorrhage during a surgical intervention.

Even though it has not been found in the bibliography any attempt to develop a computer vision algorithm to detect bleeding or blood in laparoscopic intervention while writing this article, it does exist a large bibliography focus on the visual detection of a bleeding through computerized tomography [8,9] and the development of classifiers algorithms for the images obtained by an wireless capsule endoscopic (WCE) aimed to detect haemorrhages in the gastrointestinal tract. Authors based the segmentation and classification of the pixels on the features extracted using the HVS colour model [10,11], a two-stage saliency map extraction method [12] or a simple threshold for the global ratios B/R and G/R in the BGR colour model [13].

The objective of this paper is to describe the design and implementation of a computer vision algorithm capable of analyse in real time the video provided by a laparoscopic camera and detect both the presence of blood pools and the beginning of a major bleeding. Once this goal is achieved, the algorithm can be useful for monitoring the surgical field searching for complications that may not have been detected by the surgical team or even integrated into the control system of a future autonomous surgical platform.

2. Materials and methods

2.1. Experimental material

The analysis of the images is carried out using the open source computer vision and machine learning software library OpenCV [14] and tools provided by the framework ROS (Robot Operating System) [15], in order to integrate the algorithm into a robotic platform which works using the same system. OpenCV is a computer vision library which provides of basic and advanced functionalities, such as draw a line, change the colour space of an image or apply a noise filter. ROS is a collection of software frameworks which provide with functionalities focused on robot development, and since their first versions, the OpenCV libraries are integrated into this middleware in such a way the ROS nodes can use the functionalities of this asset with just the inclusion of the proper header file.

For developing and testing our algorithm we have used two different dataset. The first dataset is composed of 23 videos of real laparoscopic surgeries recorded using a camera manned by a member of the surgical team and show diverse operations including cholecystectomies, pelvic surgeries, total mesorectal excisions, radical hysterectomies, pancreatectomy, gastrectomy, aortic lymphadenectomy, retroperitoneal dissections, nephroureterectomies and colectomies. This data set contains 17 videos that show bleeding (mean duration of 51 s) and six videos that show no bleeding (mean durations of 33 min and 31 s).

The other dataset is composed of videos of in vitro bleeding recorded in our setup using a mobile camera and independent sources of light, carried by miniature robots magnetically attached to the inner wall of the setup upper lid and externally controlled by a robotic arm. For this test we used an artificial blood composed of water, glycerine and red and black dyes, pumped by a small water pump placed out of the setup (Fig. 1). A stepper motor AM1020 from Faulhaber provides the tilt turn of the camera and all the mini robots are remotely controlled through an Arduino Mega board. Al these devices and their communications were proposed and descripted previously [16,17].

To record the second dataset five different configurations were used, recording 15 tests for each configuration. Each configuration has a different position and view angle for the camera, different number and positions of the light sources and a different amount of false blood spotted tissue were used (tissues stained with fake blood and placed around the receiving reservoir), which represent the interior of the patient.

Some images have been extracted from each dataset showing different states of a bleeding. In order to calculate the effectiveness of the algorithm, a binary map was created for each extracted image as ground truth, classifying pixels in blood and background.

2.2. Methods: blood pixel classification

First of all, Tonmoy Ghosh's [13] and Yixuan Yuan's [12] algorithm were checked analysing a few images of in vivo bleedings. These algorithms were obtained from the reference papers and they were implemented by the authors. In spite of their good results classifying blood and non-blood images from a wireless endoscopy capsule, these algorithms are not designed to work on images with a high red level, so that the results for the in vivo images were not satisfactory because the algorithm wrongly classified some tissue pixels (i.e., liver pixels) as blood pixels, resulting of a lowering of the specificity. Fig. 2 shows an example of this problem. It was also observed the red level of the pixels that belongs to blood being expelled through an incision have a more intense red colour if the illumination is adequate. Due to the results of the test it was concluded that it is needed an adaptive and dynamic classifier able to correctly segment the image without detecting background pixels as blood pixels, more restrictive when the frame has a high red level average and aimed to maintain as low as possible the false positive rate.

After analysing a series of images from real surgeries, it was observed a relationship between the individual ratios B/R and G/R of each pixel and the global ratios B/R and G/R of the frame respectively, with an increase of individual ratios proportional to the increase of the overall ratios. The individual ratios were calculated by dividing the green or blue channel of a pixel between the red channel of the same pixel. The overall ratios were calculated as the result of dividing the sum of all levels of the green or blue channels of all the pixels, between the sum of levels of the red channel of all the pixels, all measured in the BGR colour space. The relation was quantified using the k-means clustering method and optimized through a 4-fold cross-validation applied on the previously mentioned series of images to obtain a threshold Eq. (1) which separates the blood and non-blood pixels.

$$\text{Threshold}_{\text{ratio}} = 0'661 \cdot \text{Frame}_{\text{ratio}} + 0'0084 \quad (1)$$

Using these dynamics thresholds, the images were analysed again classifying as blood pixel if both individual pixel ratios were below the calculated threshold. After the classification, some morphological transformations of erode and dilation were implemented in order to remove little groups of pixels impossible to belong to a blood puddle.

2.3. Methods: haemorrhage detection

Once the algorithm performs a segmentation of the image extracting the possible blood pixels, the obtained parameters were used to implement the detection of the haemorrhage through an analysis of the values versus time of both the percentage of blood pixels as the global ratios B/R and G/R. A great variation of the analysed parameters was observed approximately during the following one second after the beginning of the bleeding, therefore it arises that the information needed to detect bleeding can be

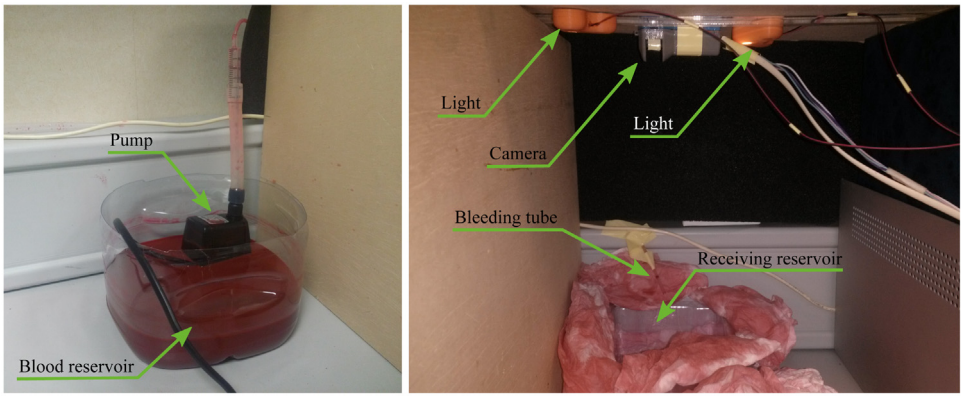

Fig. 1. Experimental setup used for the in vitro tests.

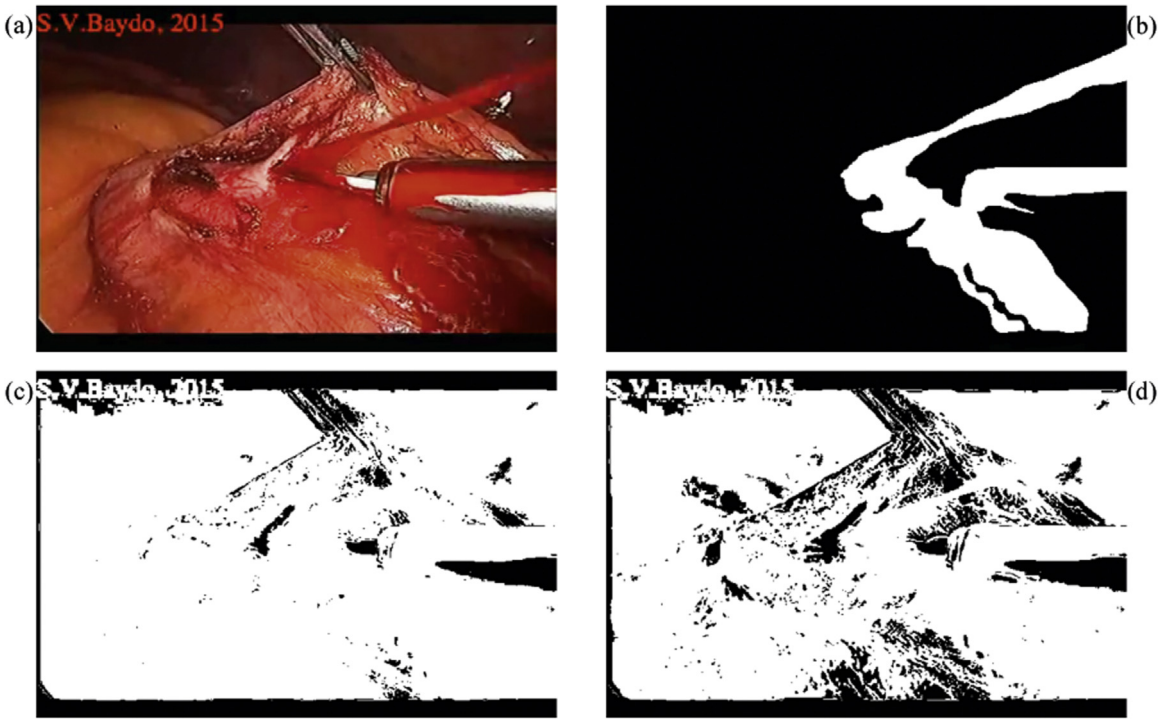

Fig. 2. Image extracted from a real surgical intervention (a), Ground truth (b), image analysed using Tonmoy Ghosh's algorithm (c) and Yixuan Yuan's algorithm (d).

obtained from the following 20 frames after the onset of bleeding (the choice of the number of frames to analyse was based on the use of videos with a ratio of 24 frames per second), comparing the analysed parameters with a series of thresholds.

It was found that the movement of the camera or the gases emitted when using a laparoscopic electrocautery sometimes causes an excessive variance of the analysed parameter not related to a bleeding. In order to solve this problem the algorithm was modify to discard the parameters of a frame with high variance compared to the previous frame, assuming that there has been a shake of the camera rather than the sudden appearance of massive bleeding. Nevertheless, the blood/non-blood pixel classification is not affected by this problem due to the frame-by-frame design of this process.

After a thorough analysis we concluded that black, blue and green pixels quite rarely represent blood being expelled through an injury. Usually they are light reflections, part of the surgical tools or belong to the black area surrounding the circular region of the image due to de optic's shape. Several tests were carried out in order to analyse the influence of these pixels on the algorithm's performance, concluding that if those pixels are not analysed then the algorithm will slightly worsened its performance but at the same time will slightly improve the time needed for the analysis, which depends of the quality of the image and the size of the black surrounding area.

The complete proposed algorithm is described in Fig. 3.

2.4. Methods: performance measurement

Three parameters were calculated to obtain a measure of the performance of the analysed algorithms as a binary classification test: accuracy, sensitivity and specificity, which are calculated according to the following equations:

$$\text{Accuracy} = \frac{\text{True Positives} + \text{True Negatives}}{\text{True Positives} + \text{True Negatives} + \text{False Positives} + \text{False Negatives}} \quad (2)$$

$$\text{Sensitivity} = \frac{\text{True Positives}}{\text{True Positives} + \text{False Negatives}} \quad (3)$$

$$\text{Specificity} = \frac{\text{True Negatives}}{\text{True Negatives} + \text{False Positives}} \quad (4)$$

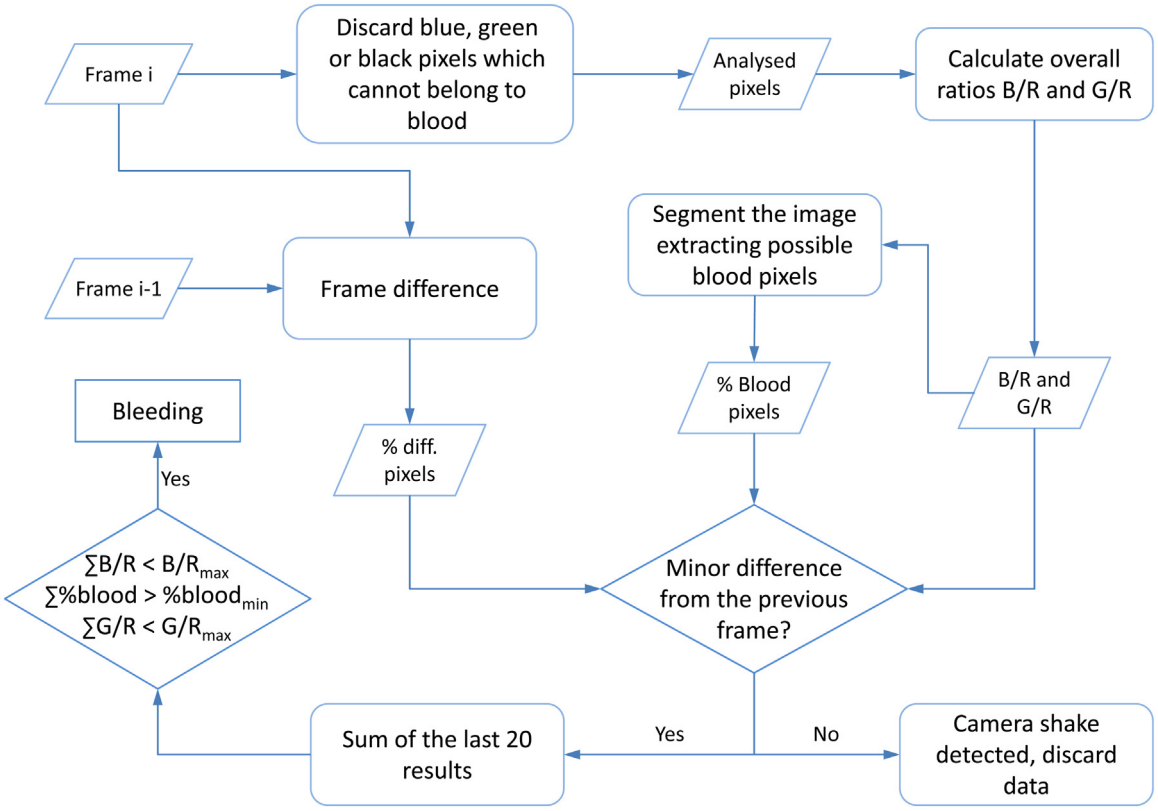

Fig. 3. Scheme of the proposed bleeding detector algorithm.

The parameters were obtained through a pixel-based comparison, therefore the True Positives are the blood pixels correctly detected as blood, the True Negatives are background pixels correctly detected as no blood, the False Positives are background pixels wrongly detected as blood and the False Negatives are the blood pixels wrongly detected as background. The sensitivity measures the amount of blood pixels correctly detected, the specificity measures the amount of background pixels correctly detected and the accuracy measures the global effectiveness of an algorithm.

3. Experimental tests

3.1. Blood pixel classification results

A first experiment was designed to evaluate the blood pixel classification capability of each algorithm through an analysis of both dataset, in vitro and in vivo images. The results are shown in Table 1 with the average of the comparison parameters. The experiment was conducted on 25 in vitro images extracted from 20 different videos and 32 in vivo images extracted from 23 different videos, so a total of 52 images (some of them did not show blood) were analysed with each algorithm.

Even though the three methods have a good performance when applied to the in vitro images, the results are poor with a low specificity when applying Tonmoy Ghosh and Yixuan Yuan methods to the in vivo images, because the algorithms wrongly classified some tissue pixels (i.e., liver pixels) as blood pixels. The algorithm proposed in this paper obtains a mediocre sensitivity value, but this is due in part to the modification made to Eq. (1) to obtain a more restrictive dynamic threshold and thus to keep the number of false positives detected low, which allows to obtain a good specificity value. In images with a surgical environment completely blood stained, it can be seen the benefits of the dynamic threshold, detecting the pixels which belong to the blood flowing from an incision which often have higher levels of red (Fig. 4).

3.2. Haemorrhage detection results

Once validated the classification of the blood pixels, the threshold of the bleeding detection parameters were calculated through an analysis of the in vitro videos measuring the first 20 frames after the first frame of the bleeding. As mentioned before, 15 tests were analysed for each one of the five different configurations, calculating the average of the minimum and maximum variation of the analysed parameters (Table 1).

Finally the videos of the in vivo test suite were analysed, trying different values for comparative thresholds (min B/R variation, min G/R variation and max blood variation for the last 20 frames) and seeking to maximize the specificity, that is, reducing the false positives when classifying the videos in “shows bleeding” or “not shows bleeding”. The best results were obtained discarding the frames with at least half of the pixels different respect the previous frame, detecting sudden sake of the camera. Using as detection conditions that the sums of B/R and G/R variations during the last 20 frames must keep below −0.08 and the sum of the blood percentage variation during the last 20 frames must keep over 10, the analysis of the videos obtained an accuracy of 78.26%, a sensitivity of 76.47% and a specificity of 83.33%. For this analysis, a true positive was achieved when the algorithm correctly detected a bleeding right after the blood start pouring from the injury, a true negative was achieved when the algorithm did not detect any bleeding in a “non-bleeding video”, a false negative was achieved when the algorithm did not detect any bleeding in a “bleeding video” and finally a false positive was achieved when: the algorithm detected a bleeding in a “non-bleeding video”, detected a bleeding in a “bleeding video” before it occurs or after the pouring due to a non-related cause (Table 2).

Table 1
Performance comparison for blood pixel classification.

		Tonmoy Ghosh	Yixuan Yuan	Our method
In vitro	Accuracy	92.25%	84.45%	95.41%
	Sensitivity	96.40%	99.64%	87.74%
	Specificity	92.09%	83.30%	96.48%
In vivo	Accuracy	60.44%	61.10%	88.96%
	Sensitivity	91.38%	93.14%	72.97%
	Specificity	48.57%	50.28%	93.41%

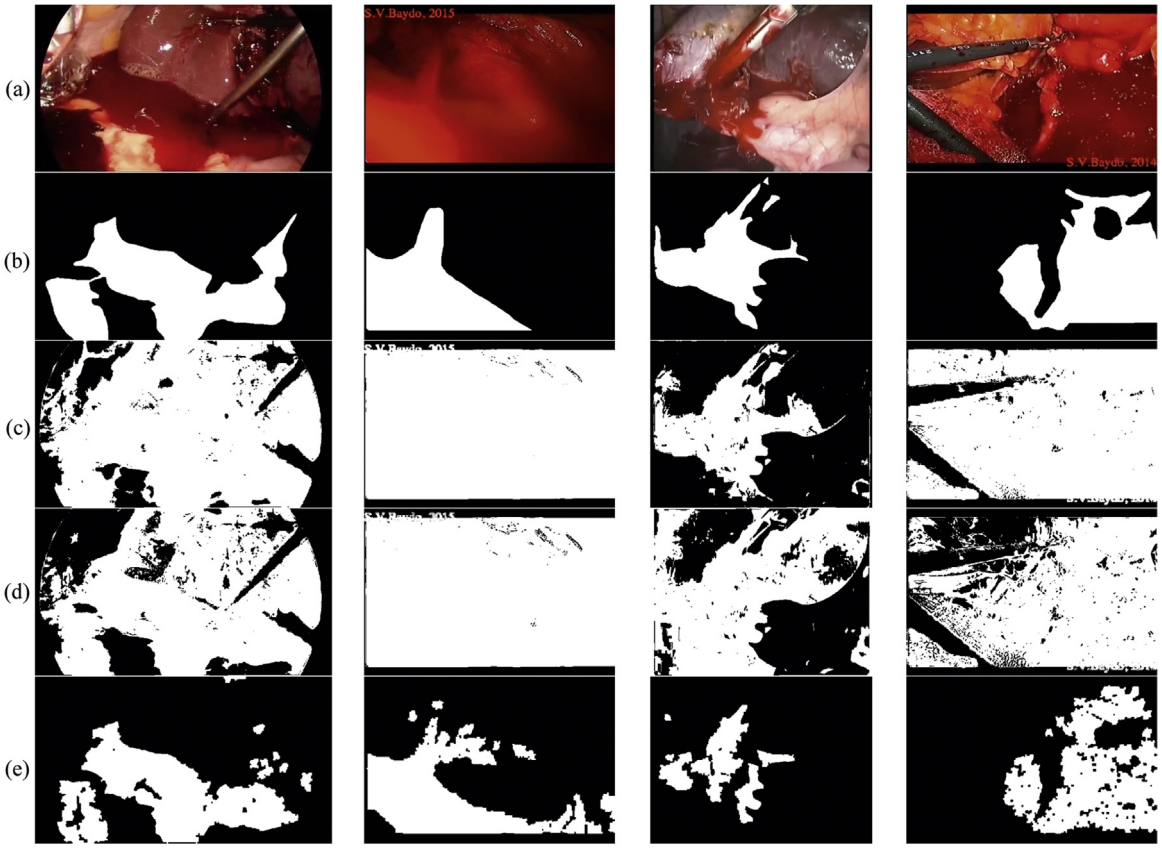

Fig. 4. Some examples of the results. (a) Original image, (b) ground truth, (c) Tonmoy Ghosh's results, (d) Yixuan Yuan's results, (e) our algorithm's results.

Table 2
Parameters of the 20 first frames after the beginning of the haemorrhage.

	Min B/R variation	Min G/R variation	Max blood variation
In vitro conf. A	−0.066	−0.0697	11.3254
In vitro conf. B	−0.1571	−0.1579	15.5642
In vitro conf. C	−0.1225	−0.1088	13.0489
In vitro conf. D	−0.089	−0.0702	11.5687
In vitro conf. E	−0.1082	−0.077	10.6634
Total average	−0.1086	−0.0967	12.4341

4. Discussions and conclusions

Nowadays, haemorrhages remain one of the major complications present in MIS interventions and the visual limitations imposed by the use of a traditional laparoscopic camera hinder its detection and treatment, increasing the risk for the patient. In this document the first steps for the design of a bleeding detector algorithm are presented, an algorithm able to work using only the images directly captured by a laparoscopic camera, obtaining acceptable results as a first approach. The successful of the analysis strongly depends of at least three factors that influence significantly the outcome.

Stability of the camera is one of the most important factors. A sudden movement of the camera can result in the loss of information needed to detect bleeding or a false positive due to a significantly increasing of the level of red when entering the frame a reddish tissue. An unmanned vision system, for example controlled by a robot as proposed in [17], will not suffer this issue and can become a reliable system for detecting bleeding.

The use of an electrocautery is very harmful for detecting bleeding using the proposed method in this paper because the gases emitted hide the blood, making hard to detect a haemorrhage only with a visual analysis but easy to solve with a correct control of the emptying of the gases.

The illumination is the most important factor, as a direct light on a blood stained surface will create some white reflections that the algorithm is not able to recognize as blood. Using an independence source light as proposed in [17] allow the surgical team to positioning it and avoid the reflections.

As a future work the algorithm requires an optimization to increase its effectiveness, for example enhancing the classification of pixels against light variations. Another possibility is to merge this algorithm with a surgical gauze detector algorithm described in [18], since both elements are strongly associated.

Acknowledgements

We thank Mr. S. V. Baydo to grant us permission to use their videos for this project.

Authors would like to thank the economic support of Spanish National Research Council through DPI2013-47196-C3-2-R project.

References

[1] Kaushik R. Bleeding complications in laparoscopic cholecystectomy: incidence, mechanisms, prevention and management. J Minim Access Surg 2010;6:59–65, http://dx.doi.org/10.4103/0972-9941.68579.

[2] Opitz I, Gantert W, Giger U, Kocher T, Krähenbühl L. Bleeding remains a major complication during laparoscopic surgery: analysis of the SALTS database. Langenbeck's Arch Surg 2005;390:128–33, http://dx.doi.org/10.1007/s00423-004-0538-z.

[3] Akaraviputh T, Opasanon S. Major vascular injury in laparoscopic cholecystectomy. Thai J Surg 2011;32:41–4.

[4] Duca S, Bălă O, Al-Hajjar N, Lancu C, Puia IC, Munteanu D, et al. Laparoscopic cholecystectomy: incidents and complications. A retrospective analysis of 9542 consecutive laparoscopic operations. HPB (Oxford) 2003;5:152–8, http://dx.doi.org/10.1080/13651820310015293.

[5] Stinton LM, Shaffer EA. Epidemiology of gallbladder disease: cholelithiasis and cancer. Gut Liver 2012;6:172–87, http://dx.doi.org/10.5009/gnl.2012.6.2.172.

[6] Mases A, Montes A, Ramos R, Trillo L, Puig MM. Injury to the abdominal aorta during laparoscopic surgery: an unusual presentation. Anesth Analg 2000;91:561–2.

[7] Allan M, Ourselin S, Thompson S, Hawkes DJ, Kelly J, Stoyanov D. Toward detection and localization of instruments in minimally invasive surgery. IEEE Trans Biomed Eng 2013;60:1050–8, http://dx.doi.org/10.1109/TBME.2012.2229278.

[8] Hamilton JD, Kumaravel M, Censullo ML, Cohen AM, Kievlan DS, West OC. Multidetector CT evaluation of active extravasation in blunt abdominal and pelvic trauma patients. Radiographics 2008;28:1603–16, http://dx.doi.org/10.1148/rg.286085522.

[9] Willmann JK, Roos JE, Platz A, Pfammatter T, Hilfiker PR, Marincek B, et al. Multidetector CT: detection of active hemorrhage in patients with blunt abdominal trauma. Am J Roentgenol 2002;179:437–44, http://dx.doi.org/10.2214/ajr.179.2.1790437.

[10] Lau PY, Correia PL. Detection of bleeding patterns in WCE video using multiple features. 2007 29th Annu. Int. Conf. IEEE Eng. Med. Biol. Soc., vol. 2007. 2007. p. 5601–4, http://dx.doi.org/10.1109/IEMBS.2007.4353616.

[11] Giritharan B, Yuan Xiaohui, Liu Jianguo, Buckles B, Oh JungHwan, Tang Shou Jiang. Bleeding detection from capsule endoscopy videos. In: 2008 30th Annu. Int. Conf. IEEE Eng. Med. Biol. Soc. 2008. p. 4780–3, http://dx.doi.org/10.1109/IEMBS.2008.4650282.

[12] Yuan Y, Li B, Meng MQ-H. Bleeding frame and region detection in the wireless capsule endoscopy video. IEEE J Biomed Heal Informatics 2016;20:624–30, http://dx.doi.org/10.1109/JBHI.2015.2399502.

[13] Ghosh T, Fattah SA, Wahid KA. Automatic bleeding detection in wireless capsule endoscopy based on RGB pixel intensity ratio. In: 2014 Int. Conf. Electr. Eng. Inf. Commun. Technol. 2014. p. 1–4, http://dx.doi.org/10.1109/ICEEICT.2014.6919173.

[14] OpenCV | OpenCV n.d. http://opencv.org/(accessed May 28, 2016).

[15] ROS.org | Powering the world's robots n.d. http://www.ros.org/(accessed May 28, 2016).

[16] Garcia-Martinez A, Lledo LD, Badesa FJ, Garcia N, Sabater-Navarro JM. Integration of heterogeneous robotic systems in a surgical scenario. In: 5th IEEE RAS/EMBS Int. Conf. Biomed. Robot. 2014. p. 24–7, http://dx.doi.org/10.1109/BIOROB.2014.6913746.

[17] Garcia-Martinez A, Mora R, Juan CG, Compan AF, Garcia N, Sabater-Navarro JM. Toward an enhanced modular operating room. In: 2016 6th IEEE Int. Conf. Biomed. Robot. 2016. p. 413–7, http://dx.doi.org/10.1109/BIOROB.2016.7523662.

[18] Garcia-Martinez A, Juan CG, Garcia NM, Sabater-Navarro JM. Automatic detection of surgical gauzes using Computer Vision. In: 23rd Mediterr. Conf. Control Autom. 2015. p. 747–51, http://dx.doi.org/10.1109/MED.2015.7158835.